J Am Oil Chem Soc (2008) 85:591–598
DOI 10.1007/s11746-008-1241-y

ORIGINAL PAPER

Phase Transition of Sunflower Oil as Affected by the Oxidation Level

Sonia Calligaris · Gianmichele Arrighetti · Luisa Barba · Maria Cristina Nicoli

Received: 5 November 2007 / Revised: 17 March 2008 / Accepted: 14 April 2008 / Published online: 9 May 2008

Abstract The influence of the oxidation level on the phase transition behavior of sunflower oil was evaluated by differential scanning calorimetry (DSC) and synchrotron X-ray diffraction (XRD) at both small and wide angles. The crystallization was monitored at a cooling/heating rate of 2 °C/min from 20 to −80 °C and vice versa applying both techniques. The triacylglycerols organize in two double-chain length structures: α 2*L* (61.87 Å) and β′ 2*L* (82.89 Å). The crystalline structure changes upon oxidation. In particular, the intensity of the XRD peak associated with the double-chain structure of β′, as well as its crystallization and melting enthalpy, significantly decreases as the oxidation level increases.

Keywords Sunflower oil · DSC · X-ray diffraction · Phase transition · Oxidation

Introduction

Lipid crystallization is of a great concern for the food industry. It plays an important role not only in the manufacturing of plastic fats, but also in the separation process of specific components from natural plant sources [1]. The lipid physical state was recently shown to affect the kinetics of lipid oxidation [2–5]. Calligaris et al. [3–5] reported that the occurrence of lipid crystallization caused a positive deviation from the Arrhenius equation leading to higher than expected oxidation rates; it was suggested that this effect could be attributed to an increment in local viscosity and reactant concentration in the liquid phase surrounding fat crystals. In general, the effect of the occurrence of phase transitions of crystallizing lipids on the oxidation rate has received very little attention and a clear understanding of the relationship between lipid oxidative stability and lipid polymorphism is lacking.

The phase transition and the polymorphisms of pure triacylglycerols (TAGs) and their mixtures has been widely studied [1, 6, 7]. There are three typical organizations for lateral packing, called α, the least stable form, β′, the metastable form, and β, the most stable polymorph. The crystal structures could present a longitudinal stacking with double- or triple-chain lengths.

Polymorphism in complex lipids is more complicated; the presence of a number of different TAGs causes the coexistence of different fat crystals including mixed crystals, which could undergo polymorphic transformations as a consequence of temperature changes [8]. Among natural lipids, the physical properties of vegetable oils have been studied to a lesser extent probably because they are liquid at room temperature although they may be partly crystalline in chilled and frozen food formulations, such as ready-to-eat meals.

The phase transitions of lipids have been mainly evaluated by means of thermo-analytical techniques, among which differential scanning calorimetry (DSC) is the most widely used. On the basis of the information supplied by DSC analysis, some authors proposed DSC as a reliable tool for the evaluation of the extent of oxidation of vegetable oils [9–11]. However, it is usually difficult or impossible to assign structural changes to DSC peaks from mixed lipids without the aid of techniques such as X-ray

S. Calligaris (✉) · M. C. Nicoli
Department of Food Science, Universitiy of Udine,
via Sondrio 2, 33100 Udine, Italy
e-mail: sonia.calligaris@uniud.it

G. Arrighetti · L. Barba
Institute of Crystallography, National Council of Research,
ss 14 km 163.5, 34012 Basovizza, Italy

diffraction (XRD) [1]. By combining results from XRD with those of DSC analysis, a set of detailed information of lipid phase transition can be obtained [12–14].

In the present study, the polymorphism and phase transition behavior of sunflower oil samples with different levels of oxidation were investigated at a cooling/heating rate of 2 °C/min from 20 to −80 °C and vice versa by means of both XRD and DSC techniques.

Materials and Methods

Materials

Sunflower oil, purchased in a local market, was used. Aliquots of 3 g of oil were inserted in 10-mL capacity vials, sealed with butyl septa and metallic caps. Samples were stored in an oven (Salvis Thermo center, Oakton, Vernon Hills, IL, USA) at 60 °C (±1 °C) in the dark for up to 13 days. At different time intervals (0, 3, 6, 10 and 13 days), samples were removed from the oven and divided into two aliquots: the first one was allowed to equilibrate at room temperature and immediately analyzed for calorimetric analysis, peroxide value (PV) and hexanal in the headspace; the second one was deep frozen at −40 °C to maintain its oxidation level and analyzed the day after by means of the XRD technique.

Methods

Quality Characteristics of Oil Samples

Peroxide values and fatty acid (FA) composition of the oil samples were measured according to the European Official Methods of Analysis [15].

Oxidative stability was determined by the Rancimat test at 100 °C with an air flow of 20 L/h using a mod. 679 Metrohm Rancimat (Metrohm, Herisau, Switzerland).

Measurement of Hexanal by Static Headspace GC

Hexanal concentration was measured by static headspace GC. A HGRC Mega 2 Series gas chromatograph (Fisons Instruments, Milan, Italy) equipped with a headspace sampler (Carlo Erba HS 250; Carlo Erba Strumentazioni, Milan, Italy) and a thermal conductivity detector (Fisons HWD Control, Fisons Instruments, Milan, Italy) was used. Hexanal was separated isothermally at 80 °C using a glass column (2 m × 2 mm) packed with 6.6% a Carbowax 20M on Carbopack B 60–80 mesh. The GC conditions were as follows: sample temperature, 35 °C; injector and detector temperature, 180 °C; nitrogen flow rate, 35 L/min. Before analysis, samples were stored at 35 °C for 40 min in a temperature control bath to reach equilibrium conditions. The chromatograms were integrated using Chromcard (Ver. 1.18, 1996; CE Instrument, Milan, Italy) chromatography data system software.

Calorimetric Analysis

Calorimetric analysis were carried out using a TA4000 differential scanning calorimeter (Mettler-Toledo, Greifensee, Switzerland) connected to a GraphWare software TAT72.2/5 (Mettler-Toledo, Greifensee, Switzerland). Heat flow calibration was achieved using indium (heat of fusion 28.45 J/g). Temperature calibration was carried out using hexane (m.p −93.5 °C), water (m.p. 0.0 °C) and indium (m.p. 156.6 °C). Samples were prepared by carefully weighing 10–15 μg of the material in 20-μL aluminum DSC pans, closed without hermetic sealing. An empty pan was used as a reference. Samples were heated under nitrogen flow (10 mL/min) at 40 °C for 15 min to erase the crystallization memory, cooled to −80 °C and then heated from −80 to 20 °C. It should be noted that the heating does not modify the oxidation level of samples. The scanning rate was 2 °C/min. The start and the end of melting transition were taken as on-set (T_{on}) and off-set (T_{off}) points of transition, that are the points at which the extrapolated baseline intersects the extrapolated slope of the curve. The T_{peak} corresponds to the peak maximum temperature. Results were normalized to account for the weight variation of the samples. Total peak enthalpy of crystallization (ΔH_{cr}) and melting (ΔH_{m}) was obtained by integration. The program STAR ever. 8.10 (Mettler-Toledo, Greifensee, Switzerland) was used to plot and analyze the thermal data.

X-Ray Diffraction

X-ray diffraction patterns were recorded at the XRD beamline 5.2 at the Synchrotron Radiation Facility Elettra located in Trieste (Italy). The X-ray beam emitted by the wiggler source on the Elettra 2 GeV electron storage ring was monochromatized by a Si(111) double crystal monochromator, focused on the sample and collimated by a double set of slits giving a spot size of 0.2 × 0.2 mm. A drop of oil was lodged into a nylon pre-mounted 20 μm cryoloop for crystallographic experiments (loop diameter 0.7–1.0 mm) (Hampton Research HR4-965, Aliso Viejo, CA, USA). Sample temperature was controlled by means of a 700 series cryocooler (Oxford Cryosystems, Oxford, UK) with an accuracy of ∼1 °C. The temperature profile was the same of the DSC experiments (heating at 40 °C for 15 min, cooling to −80 °C and then heating to 20 °C at a scanning rate of 2 °C/min). Data were collected at a photon energy of 7.72 KeV ($\lambda = 1.6044$ Å), using a 165 mm CCD-based X-ray detector system (MarCCD)

(Marresearch GmbH, Norderstedt, Germany). As the intensity of the synchrotron radiation beam slowly decreased during the experiment, every diffraction pattern was collected rotating the sample for 0.02 degrees at variable rotation speed, under the condition that the dose of photons absorbed by the sample was the same for every pattern. Several hundred bidimensional patterns collected with the MarCCD were calibrated and integrated using the software FIT2D [16] obtaining several series of powder-like patterns, one for every oil sample experiment. The high brilliance source allowed us to make the analysis of weak structures not otherwise detectable, which helped in the process of indexing the patterns.

Peaks positions of the XRD patterns obtained by the crystalline phases were found by means of the program Winplotr [17]. Cell parameters were obtained using the program CHECKCELL [18]. Indexing was performed on a single pattern, chosen in proximity of peak *B* of DSC, at a temperature of −57 °C in order to observe in the same pattern both the α-form peaks and the β'-form. When we mention reticular parameter *c*, we always refer to the value obtained at this temperature.

Data Analysis

All determinations are expressed as the mean ± standard deviation of at least three measurements from two experiment replications. One-way analysis of variance was carried out, and significance between means was determined using the Tukey test (JMP 3.2.5, SAS Institute Inc., Cary, NC, USA). Data reported in the figures refer to a single experiment set, but they are representative of the entire set of data. Linear regression analysis by least squares regression was performed by S-PLUS (Insightful Corporation, Seattle, WA, USA, ver. 7, 2004). The goodness of fit was evaluated on the basis of statistical parameters of fitting (R^2, *P*) and the residual analysis.

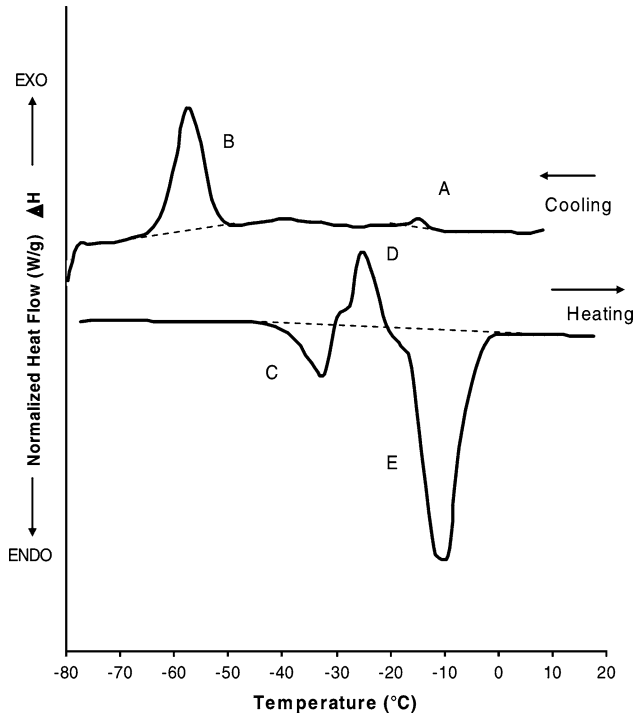

Fig. 1 Cooling and heating DSC thermogram of sunflower oil obtained at a scanning rate of 2 °C/min from 20 to −80 °C and vice versa

Results and Discussion

Chemical and Physical Characteristics of Sunflower Oil

Table 1 shows the FA composition and oxidation indices of the fresh un-oxidized sunflower oil used in the present research. The DSC results obtained by cooling the oil at 2 °C/min from 20 to −80 °C and then heating it from −80 to 20 °C at the same scanning rate are reported in Fig. 1. The cooling DSC curve presents two exothermic peaks (*A*–*B*) associated with two distinct crystallization events. The first one appears at $T_{on} = -11.5 \pm 0.2$ °C and can be attributed to the phase transition of a small oil fraction containing mainly saturated FAs such as palmitic and stearic acid. The second exothermic peak has been shown at $T_{on} = -51.1 \pm 0.2$ °C corresponding to the phase transition of the low-melting highly unsaturated oil fraction. During heating, DSC curve shows one endothermic peak (*C*) at $T_{on} = -37.8 \pm 0.3$ °C followed by an exothermic one ($T_{on} = -31.5 \pm 0.2$) (*D*). This probably indicates that a portion of the crystals formed during cooling melts and re-crystallizes into more stable

Table 1 Qualitative characteristics and fatty acid composition of sunflower oil

Determination	
Oxidation indexes	
PV (mequiv O_2/kg_{oil})	2.4 ± 0.6
Induction time (h)[a]	12.6 ± 0.8
FA composition	
$C_{16:0}$	6.83 ± 0.20
$C_{18:0}$	3.03 ± 0.02
$C_{18:1}$	34.23 ± 0.40
$C_{18:2}$	55.38 ± 0.50
$C_{20:0}$	0.18 ± 0.02
$C_{20:1}$	0.15 ± 0.02
$C_{22:0}$	0.15 ± 0.03

[a] Induction time to oxidation at 100 °C measured by the Rancimat test apparatus

polymorphic structures. Finally, the further temperature increase causes the progressive melting of all the crystals (peak *E*, $T_{on} = -16.5 \pm 0.1$ °C). At -6.8 ± 0.3 °C (T_{off} of peak E) the oil is completely melted.

X-ray diffraction patterns of un-oxidized sunflower oil recorded at wide (WAX) and small angle (SAX) as a function of temperature during cooling and further heating at 2 °C/min are shown in Fig. 2. The DSC curve was also reported in order to show the correspondence between DSC and XRD events. From 20 °C to -13.6 ± 0.1 °C (T_{peak} A) only two bumps at about 4.466 and 23.0 Å are observed. These bumps are associated with the short-range organization of the TAG molecules in the liquid phase, as previously reported by other authors [19, 20]. In fact, when fats are melted, a certain degree of order is also kept in the liquid state [19].

Upon further cooling, XRD patterns show the appearance of wide- and small-angle diffraction peaks indicating that the sunflower oil starts to crystallize. Table 2 summarizes the interplanar distances (Å) of the XRD peaks, the relevant temperature of occurrence and the corresponding DSC events. The indexing of peaks (Miller index) and the corresponding crystalline structure are also reported in the lower part of the table.

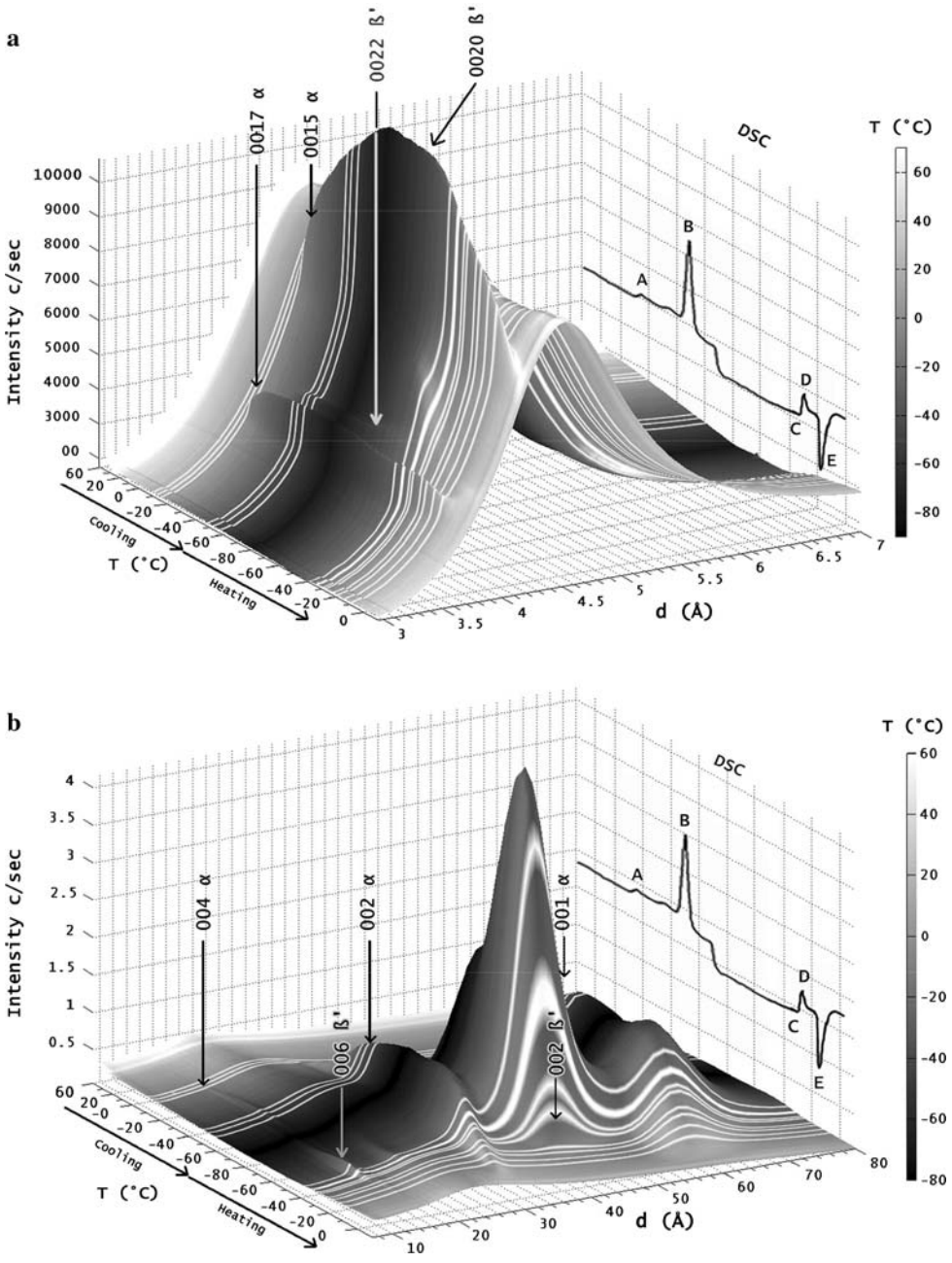

Fig. 2 Wide- (WAX) (**a**) and small-angle (SAX) (**b**) X-ray diffraction patterns as a function of temperature recorded during cooling and subsequent heating of sunflower oil at scanning rate of 2 °C/min from 20 to −80 °C and vice versa. Every diffraction pattern is represented as intensity (counts) vs. interplanar distances *d* (Å) as a function of temperature. As the temperature decreases the patterns present a darker color. The patterns recorded in correspondence of T_{on}, T_{peak} and T_{off} of DSC thermal events are represented with *white lines*. For comparison DSC curve are also reported

Table 2 Interplanar distances of wide and small angle diffraction XRD peaks, measured in correspondence of relevant temperatures of DSC curve. Reticular parameters and Miller indices of each peak are assigned in the lower part of the Table

Temperature (°C) and DSC event	Interplanar distances (Å)											
	Wide-angle					Small-angle						
-13.6 ± 0.1 T_{peak} A						4.466 ± 0.001			23.0 ± 0.1			
-16.8 ± 0.1 T_{off} A	3.6955 ± 0.0005		4.159 ± 0.005			4.4598 ± 0.0004		15.7 ± 0.1	23.1 ± 0.6	29.3 ± 0.7		58.3 ± 4.0
-54.8 ± 0.2 T_{peak} B	3.6655 ± 0.0002	3.750 ± 0.003	4.1207 ± 0.0002	4.1673 ± 0.0001	4.3524 ± 0.0003	13.92 ± 0.04		16.11 ± 0.02	24.9 ± 0.5	31.5 ± 0.5	42.1 ± 1.1	62.0 ± 1.1
-32.9 ± 0.3 T_{peak} C	3.6843 ± 0.0002	3.902 ± 0.003	4.1397 ± 0.0002	4.1879 ± 0.0001	4.3753 ± 0.0003	14.13 ± 0.02		15.5 ± 0.2	21.2 ± 0.1	30.8 ± 0.9	42.0 ± 3.2	61.1 ± 8.2
-25.3 ± 0.3 T_{peak} D	3.6921 ± 0.0003		4.1468 ± 0.0004		4.401 ± 0.001	14.186 ± 0.003		15.3 ± 0.2	21.8 ± 0.8	30.4 ± 0.2	42.0 ± 0.1	60.0 ± 4.3
-11.9 ± 0.1 T_{peak} E	3.7213 ± 0.0005		4.1647 ± 0.0002		4.453 ± 0.001	14.15 ± 0.05		15.0 ± 0.2	24.4 ± 0.8	29.6 ± 0.2	39.8 ± 0.1	59.4 ± 4.4
Miller index												
α-form hexagonal $c = 61.87$ Å	0 0 17		0 0 15		Amorphous			0 0 4	Amorphous	0 0 2		0 0 1
β'-form monoclinic or orthorhombic $c = 82.89$ Å		0 0 22		0 0 20			0 0 6				0 0 2	

The first XRD peaks appear at -16.8 ± 0.1 °C (T_{off} A) at wide (3.69; 4.16 Å) (Fig. 2a) and small angle (15.7, 29.3, 58.3 Å; Fig. 2b). These XRD peaks overlap the amorphous matrix signal that, as shown in the Table 2, is observed during all the experiments. The new peaks are identified as reflections 0 0 17, 0 0 15, 0 0 4, 0 0 2 and 0 0 1 of the metastable α-form with a reticular parameter of 61.87 Å, which corresponds to the organization of the TAGs in a hexagonal sub-cell. The intensity of these peaks increases as temperature decreases. During further heating, a progressive intensity decrease is recorded and the peaks disappear at -6.8 ± 0.3 °C (T_{off} peak E).

Besides the crystalline α-form evolution, the XRD pattern shows at -54.8 ± 0.2 °C (T_{peak} B) the appearance of new peaks (wide angle = 3.75, 4.17; small angle = 13.9, 42.1 Å) indexed as lines 0 0 22, 0 0 20, 0 0 6 and 0 0 2, respectively, of a double-length stacking β'-form ($2L$) with a reticular parameter of 82.89 Å (Table 2). As reported by Garti and Sato [21], the structure could be a monoclinic or orthorhombic cell related to a tighter packing of molecules. During cooling, the β' peaks increase faster than those associated with the α-form. As the temperature approaches −80 °C, the β' peaks are still increasing in intensity.

Upon further heating, the α-form slowly melts, while β'-form continues to organize probably incorporating in the crystal network the molecules melted from the α-form and/or subtracted from the amorphous phase. This event is well pointed out by the presence in DSC results of an endothermic peak (C) followed by an exothermic one (D).

It should be noted that, as reported in Table 2, all the α and β' peaks are detected from -16.8 ± 0.1 during cooling until -6.8 ± 0.3 °C during heating. The only exception are the wide-angle β' peaks that become indistinguishable from the background from -25.3 ± 0.3 °C (T_{peak} D) during heating due to their low intensity. In fact, it is not possible during heating to compute the clear position of such XRD peaks. However, the clear presence of small-angle peaks, more intense and visible due to their higher peak-to-background ratio, points out that β'-form is still present in the matrix.

Finally, β'-form disappears at -6.8 ± 0.3 °C (T_{off} peak E) and the XRD pattern shows once again only the peaks associated with the organization of TAGs in the liquid state.

Oxidation Kinetics

In order to evaluate the influence of the development of oxidation on the phase transition behavior of sunflower oil, DSC and XRD analysis has been performed on samples with different oxidation level. To obtain samples with different oxidation level, sunflower oil was incubated at 60 °C for increasing lengths of time. During storage, the

Table 3 Changes of peroxide value (PV) and hexanal peak area of sunflower oil as a function of storage time at 60 °C

Oxidation time (days at 60 °C)	Peroxide number (mequiv O_2/kg_{oil})	Hexanal peak area (arbitrary unit)
0	2.4 ± 0.6[a]	3300 ± 521[a]
3	9.7 ± 1.1[b]	13258 ± 1021[b]
6	37.8 ± 1.6[c]	58692 ± 1214[c]
10	43.5 ± 1.4[d]	124953 ± 2541[d]
13	81.7 ± 2.1[e]	147245 ± 2694[e]

Mean values in the same column with a common superscript letter are not significantly different ($P < 0.05$)

PV increases as a consequence of the reaction between oxygen and unsaturated FA (Table 3). As well known, the PV changes result from a balance between the hydroperoxides produced and those decomposed during propagation and termination steps of oxidation reactions. The decomposition of hydroperoxides leads to the formation of a number of volatile compounds, among which hexanal is one of the widely used as oxidation index. Table 3 shows the increase in the headspace concentration of hexanal during storage at 60 °C. It should be noted that besides the changes in PV and hexanal, the FA composition, as expected, does not show any significant differences (data not shown).

The DSC and XRD results of sunflower oil stored for increasing time at 60 °C show the same features as the un-oxidized ones but with some changes in the details. Figure 3 shows, as an example, the XRD patterns and DSC curve of sunflower oil stored for 13 days at 60 °C. The

Table 4 Intensity of peak 002 β' as a function of storage time at 60 °C

Oxidation time (days at 60 °C)	Peak 002 β'
0	3.85 ± 0.03[a]
3	3.17 ± 0.05[b]
6	3.15 ± 0.02[b]
10	3.12 ± 0.01[b]
13	2.50 ± 0.04[c]

Mean values in the same column with a common superscript letter are not significantly different ($P < 0.05$)

XRD patterns of oxidized oil do not differ with those of the un-oxidized one in terms of peak position. The only changes observed concern the peak intensity. In order to compare the XRD data, the intensity of the peaks in XRD pattern were normalized to the maximum intensity of peak 0 0 1 of α-form (lower θ angle peak) ($d = 61.4$ Å; normalized intensity 1.0). The only significant difference ($P < 0.05$) in the peak intensity upon oxidation is the intensity decrease of the peak 0 0 2 β' ($2L$ at 42.1 Å), as shown in Table 4. It should be remembered that this peak is the most intense peak observed in the XRD patterns and it represents the main crystal form in the crystal network of un-oxidized oil.

Oxidation results also associated with the decrease in the crystallization and melting enthalpy of DSC peaks B and E from 0 to 13 days (Table 5). In addition, a slight shift in the initial crystallization temperature (T_{on} peak B) toward lower temperatures is observed while the melting temperature (T_{on} peak E) does not show significant changes. It

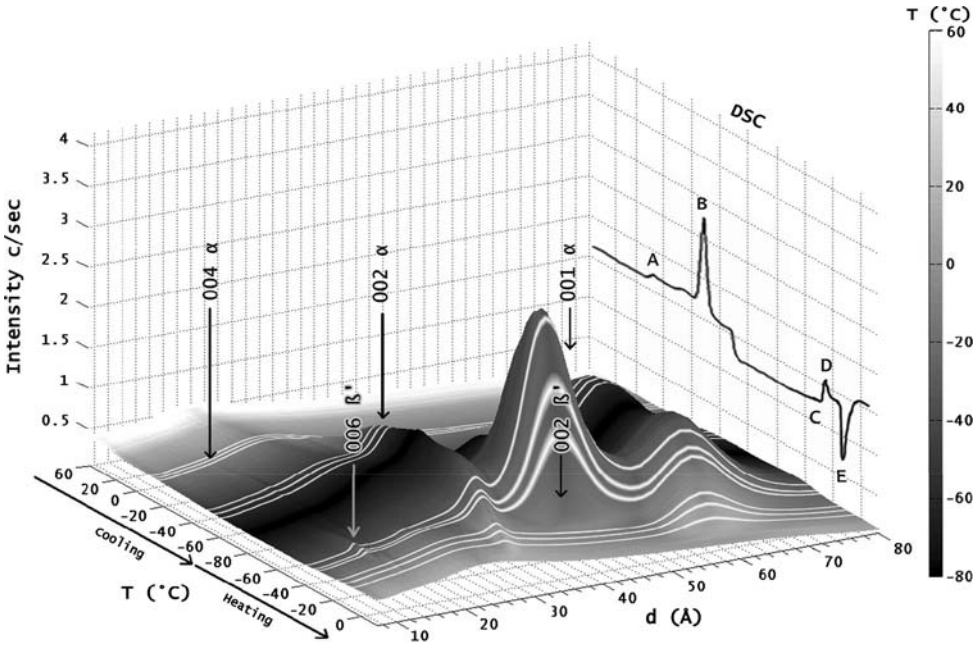

Fig. 3 Wide-angle X-ray diffraction patterns (WAX) as a function of temperature recorded during cooling and subsequent heating of sunflower oil stored at 60 °C for 13 days at scanning rate of 2 °C/min from 20 to −80 °C and vice versa. Every diffraction pattern is represented as intensity (counts) vs. interplanar distances d (Å) as a function of temperature. As the temperature decreases the patterns present a darker color. The patterns recorded in correspondence of T_{on}, T_{peak} and T_{off} of DSC thermal events are represented with *white lines*. For comparison DSC curve are also reported

Table 5 Crystallization enthalpy (ΔH_{crist}) and initial temperature of crystallization (T_{on}) associated with peak B and melting enthalpy (ΔH_m) and initial temperature of melting (T_{on}) associated with peak E of sunflower oil as a function of oxidation time

Oxidation time (days at 60 °C)	ΔH_{crist} (J/g)	T_{on} crystallization (°C)	ΔH_m (J/g)	T_{on} melting (°C)
0	29.2 ± 0.6[a]	−51.1 ± 0.2[a]	56.7 ± 0.4[a]	−16.5 ± 0.1[a]
3	28.2 ± 0.4[a]	−51.6 ± 0.1[a]	53.2 ± 0.2[b]	−16.4 ± 0.2[a]
6	26.7 ± 0.4[b]	−51.1 ± 0.3[a]	52.1 ± 0.3[b]	−16.5 ± 0.2[a]
10	24.2 ± 0.2[c]	−52.0 ± 0.3[b]	52.6 ± 0.3[b]	−16.5 ± 0.3[a]
13	24.4 ± 0.2[c]	−52.3 ± 0.2[b]	48.2 ± 0.4[e]	−16.2 ± 0.1[a]

Mean values in the same column with a common superscript letter are not significantly different ($P < 0.05$)

should be noted that these calorimetric results are similar to those reported by other authors of oil having undergone oxidation during frying [10, 11].

The differences observed in DSC and XRD results of oxidized sunflower oil could be related to the compositional changes associated with the development of oxidative reactions. As known, oxidation leads to the formation of components with higher polarity, such as hydroperoxides, and lower molecular weight (volatile compounds) than the starting TAGs [22]. In our experimental conditions, these changes are well demonstrated by the increase in PV and hexanal peak area (Table 3). The presence of charged and smaller molecules in the lipid matrix probably reduces the capacity of TAGs to align in the right way to form crystals. This hypothesis is supported by the decrease of the crystallization and melting enthalpy as well as of XRD peak 0 0 2 β' intensity. These events clearly indicate that a smaller part of the lipid matrix undergo phase transition in samples with increasing oxidation level. In addition, the decrease of crystallization temperature highlights that the undercooling needed to observe the phase transition is greater in oxidized samples indicating a higher difficulty to crystallize. At the same time, since neither new XRD peaks nor shifts in the interplanar distances appear upon oxidation, it can be inferred that the crystal structures formed in heated samples are the same as those of the un-oxidized samples. Thus, the oxidation reaction products remain in the amorphous phase and do not contribute to crystal network formation.

It is interesting to note that a good linear correlation was found between chemical oxidation indexes and physical parameters. In particular, the changes in PV are well correlated ($P < 0.05$) with the intensity at peak 42.1 Å in XRD ($R^2 = 0.93$), but also with the crystallization enthalpy of peak B and the melting enthalpy of peak E ($R^2 = 0.97$ and $R^2 = 0.85$ respectively, $P < 0.05$). A similar linear relationship is seen between the hexanal peak area and the intensity of peak at 42.1 Å ($R^2 = 0.78$), the crystallization enthalpy of peak B ($R^2 = 0.97$) and the melting enthalpy of peak E ($R^2 = 0.85$). These results indicate that the analytical techniques generally applied to study the physical properties of lipids could be also used to get an insight into their oxidative level with some interesting advantages, such as shorter experimental times, no use of solvents, very limited sample preparation and small sample size. However, further research is needed to evaluate the possibility of applying these techniques routinely.

In conclusion, the use of DSC analysis with a high-flux X-ray source for the XRD technique allows one to carry out the identification and the characterization of the crystalline structures formed in sunflower oil. In particular, the TAGs organize in two double-chain length structures: α 2L (61.87 Å) and β' 2L (82.89 Å). From a technological point of view, these structures coexist at the temperature normally applied for the frozen storage of foods (−18 °C) with the prevalence of the β'-form. It is interesting to note that in such conditions the oil is not completely crystallized as shown by the presence of an amorphous signal during the whole XRD experiment. As suggested by Calligaris et al. [3], the liquid/amorphous phase that still remain in the sunflower oil stored below 0 °C could undergo oxidation also in frozen foods.

These physical properties change upon oxidation. In particular, the intensity of the XRD peak 0 0 2 associated with the double-chain structure of β'-form, as well as its crystallization and melting enthalpy, significantly decreases as oxidation level increases.

Results obtained in this study allow us to generate detailed information on the physical state of sunflower oil with different oxidation levels as a function of temperature.

References

1. Sato K (1999) Solidification and phase transformation behavior of fats—a review. Lipids 12:467–474
2. Kristott J (2000) Fats and oils. In: Kilcast D, Subramaniam P (eds) The stability and shelf-life of food. Woodheard Publishing Limited, Cambridge, pp 25–32
3. Calligaris S, Manzocco L, Conte LS, Nicoli MC (2004) Application of a modified Arrhenius equation for the evaluation of oxidation rate of sunflower oil at sub-zero temperature. J Food Sci 69(8):E361–E366

4. Calligaris S, Manzocco L, Nicoli MC (2006) Influence of crystallization on the oxidative stability of extra virgin olive oil. J Agric Food Chem 54(2):529–535
5. Calligaris S, Manzocco L, Nicoli MC (2007) Modeling the temperature dependence of oxidation rate in water-in-oil emulsions stored at sub-zero temperatures. Food Chem 101:1019–1024
6. Hagemann JW (1988) Thermal behavior and polymorphism of acylglycerides. In: Garti N, Sato K (eds) Crystallization and polymorphism of fats and fatty acids. Marcel Dekker Inc., New York, pp 227–266
7. Lawler JL, Dimick PS (1998) Crystallization and polymorphism of fats. In: Akoh CC, Min DB (eds) Food lipids. Marcel Dekker Inc., New York, pp 229–250
8. Marangoni AG, Lencki RW (1998) Ternary phase behavior of milk fat fractions. J Agric Food Chem 46:3879–3884
9. Tan CP, Che Man YB (1999) Quantitative differential scanning calorimetric analysis for monitoring the oxidation of heated oils. J Am Oil Chem Soc 67:177–184
10. Vittadini E, Lee JH, Frega NG, Min DB, Vodovotz Y (2003) DSC determination of thermally oxidized olive oil. J Am Oil Chem Soc 80:532–537
11. Aguilera J, Gloria H (1997) Determination of oil in fried potato products by differential scanning calorimetry. J Agric Food Chem 45:781–785
12. Kellens M, Meeussen W, Riekel C, Reynaers H (1990) Time resolved X-ray diffraction studies of the polymorphic behaviour of tripalmitin using synchrotron radiation. Chem Phys Lipids 52:79–98
13. Keller G, Lavigne F, Loisel L, Ollivon M, Bourgaux C (1996) Investigation of the complex thermal behaviour of fats: combined DSC and X-ray diffraction techniques. J Therm Anal 47:1545–1565
14. Keller G, Lavigne F, Forte L, Andrieux K, Dahim M, Loisel C, Ollivon M, Bourgaux C, Lesieur P (1998) DSC and X-ray diffraction coupling. Specifications and application. J Therm Anal 51:783–791
15. European Community, Regulation 2568/91 (1991) Official Journal of European Community, pp 29–30, 64–67
16. Hammersley AP, Svensson SO, Hanfland M, Fitch AN, Hausermann D (1996) Two-dimensional detector software: from real detector to idealised image or two-theta scan. High Pressure Res 14:235–248
17. Roisnel T, Rodriguez-Carvajal J (2000) WinPLOTR: a Windows tool for powder diffraction patterns analysis materials science forum. In: Delhez R, Mittenmeijer EJ (eds) Proceedings of the seventh European powder diffraction conference (EPDIC 7), Barcelona, pp 118–123
18. Laugier J, Bochu B (2000) CHECKCELL: a software performing automatic cell/space group determination, collaborative computational project number 14 (CCP14). Laboratoire des Matériaux et du Génie Physique de l'Ecole Supérieure de Physique de Grenoble, France
19. Larsson K (1997) Molecular organization in lipids. In: Friberg SE, Larsson K (eds) Food emulsions. Marcel Dekker Inc., New York
20. Lopez C, Lavigne F, Lesieur P, Keller G, Ollivon M (2001) Thermal and structural behavior of anhydrous milk fat. 2. Crystalline forms obtained by slow cooling. J Dairy Sci 84:2402–2421
21. Garti N, Sato K (1988) Crystallization and polymorphism of fats and fatty acids. Surfactant science series, Marcel Dekker Inc., New York, vol 31, pp 9–95
22. Frankel EN (1998) Stability methods. In: Frankel EN (ed) Lipid oxidation. The Oil Press, Dundee, pp 99–114